

---

# SCALABLE DISTRIBUTED APPROXIMATION OF INTERNAL MEASURES FOR CLUSTERING EVALUATION

---

**Federico Altieri**  
University of Padova  
Padova, Italy  
altieri@dei.unipd.it

**Andrea Pietracaprina**  
University of Padova  
Padova, Italy  
capri@dei.unipd.it

**Geppino Pucci**  
University of Padova  
Padova, Italy  
geppo@dei.unipd.it

**Fabio Vandin**  
University of Padova  
Padova, Italy  
vandinfa@dei.unipd.it

## ABSTRACT

An important step in cluster analysis is the evaluation of the quality of a given clustering through structural measures of goodness. Measures that do not require additional information for their evaluation (but the clustering itself), called internal measures, are commonly used because of their generality. The most widely used internal measure is the *silhouette coefficient*, whose naïve computation requires a quadratic number of distance calculations, unfeasible for massive datasets. Surprisingly, there are no known general methods to efficiently approximate the silhouette coefficient of a clustering with rigorously provable high accuracy. In this paper, we present the first scalable algorithm to compute such a rigorous approximation for the evaluation of clusterings based on any metric distances. Our algorithm approximates the silhouette coefficient within a mere additive error  $O(\varepsilon)$  with probability  $1 - \delta$  using a very small number of distance calculations, for any fixed  $\varepsilon, \delta \in (0, 1)$ . We also provide a distributed implementation of the algorithm using the MapReduce model, which runs in constant rounds and requires only sublinear local space at each worker, thus making our estimation approach applicable to big data scenarios. An extensive experimental evaluation provides evidence that our algorithm returns highly accurate silhouette estimates, unlike competing heuristics, while running in a fraction of the time required by the exact computation.

**Keywords** Clustering, Silhouette, MapReduce, Randomization, PPS

## 1 Introduction

Clustering is a fundamental primitive for the unsupervised analysis of datasets, and finds applications in a number of areas including pattern recognition, bioinformatics, biomedicine, and data management [2]. In its more general definition, clustering requires to identify groups of elements where each group exhibits high similarity among its members, while elements in different groups are dissimilar. Starting from this common definition, several algorithms have been proposed to identify clusters in a dataset [17], often formalizing clustering as an optimization problem (based on a cost function). The resulting optimization problems are usually computationally hard to solve, and algorithms providing rigorous approximations are often sought in such cases. More recently, the focus has been on developing efficient methods that scale to the massive size of modern datasets [3, 6, 8, 9, 23, 24] while still providing rigorous guarantees on the quality of the solution.

A common step after clustering has been performed is *clustering evaluation* (sometimes called *clustering validation*). Clustering evaluation usually employs an evaluation measure capturing the goodness of the structure of a clustering. Evaluation measures are classified into *unsupervised* or *internal* measures, which do not rely on external information, and *supervised* or *external* measures, which assess how well a clustering matches the structure defined by external information [30]. While external measures are useful only when additional external knowledge regarding the cluster structure of the data is available, internal measures find applications in every scenario.

The most commonly used internal measure for clustering evaluation is the *silhouette coefficient* [28] (for brevity, called *silhouette* in this paper). The silhouette of a clustering is the average silhouette of all elements in the clusters, and, in turn, the silhouette  $s(e)$  of an element  $e$  in some cluster  $C$  is defined as the ratio  $(b(e) - a(e)) / \max\{a(e), b(e)\}$ , where  $a(e)$  is the average distance of  $e$  from the other elements of  $C$ , and  $b(e)$  is the minimum average distance of  $e$  from the elements of another cluster  $C'$ . In other words,  $s(e)$  provides an indication to what extent  $e$  is closer (on average) to elements in its cluster  $C$  than to elements in the “closest” cluster  $C' \neq C$ . The use of the silhouette for clustering evaluation is suggested by widely used data mining books [16, 30], and has found application in several important

areas [18, 26, 29, 34]. The naïve computation of the silhouette for a clustering of  $n$  elements requires  $\Theta(n^2)$  distance calculations, which is unfeasible for massive dataset that require distributed clustering solutions [4, 5, 13, 14, 23]. Surprisingly, while several methods have been proposed to efficiently cluster large datasets with rigorous guarantees on the quality of the solution, there are no methods to efficiently approximate the silhouette featuring *provably high accuracy*.

## 1.1 Related Work

While the silhouette is one of the most popular internal measures for clustering evaluation [25, 32, 35], the quadratic complexity of the naïve exact calculation makes its use impractical for clusterings of very large datasets. For this reason, some attempts have been made to propose variants that are faster to compute, or to simplify its calculation in some special cases.

Hruschka et al. [19] present the *simplified silhouette* for the evaluation of clusterings obtained on the basis of objective functions involving squared Euclidean distances (e.g.,  $k$ -means clusterings [2]). The simplified silhouette is a variant of the silhouette, where for each element  $e$  in a cluster, the aforementioned quantities  $a(e)$  and  $b(e)$  are redefined, respectively, as the (squared) distance between  $e$  and the centroid of its cluster, and of the closest centroid of another cluster. In this fashion, the complexity of the whole computation reduces to  $O(nk)$ . While Hruschka et al. [19] and Wang et al. [33] provide empirical evidence that the simplified silhouette can be an effective evaluation measure for clusterings returned by Lloyd’s algorithm [22], there is no evidence of its effectiveness for other types of clusterings (e.g. clusterings based on other distance functions) and, moreover, the discrepancy between the original silhouette and the simplified silhouette can grow very large.

Frahling and Sohler [15] proposed an optimization heuristic for speeding-up the computation of the exact silhouette for clusterings based on Euclidean distances. For each element  $e$  of a cluster  $C$ , while the term  $a(e)$  is computed according to its definition, in an attempt to reduce the operations needed to compute the term  $b(e)$ , the heuristic first determines the average distance  $d(e, C')$  between  $e$  and the elements of the cluster  $C' \neq C$ , whose centroid is closest to  $e$ , and then sets  $b(e) = d(e, C')$  in case the distance between  $e$  and the centroid of any other cluster  $C'' \notin \{C, C'\}$  is larger than or equal to  $d(e, C')$ , since in this case there is no need to compute any other average distance  $d(e, C'')$ . However, when this is not the case,  $b(e)$  must be computed according to its definition and its worst case complexity remains clearly quadratic.

The Apache Spark programming framework<sup>1</sup> provides optimized methods for computing the silhouette of clusterings under  $d$ -dimensional squared Euclidean distances and under one formulation of cosine distance. Indeed, in these specific cases, simple algebra suffices to show that precomputing, for each of the  $k$  clusters, a limited number of values dependent on the coordinates of the cluster’s points, yields a fully parallelizable algorithm featuring  $O(nkd)$  work. However, using squared distance measures to compute the silhouette tends to push the measure closer to 1 compared to linear distances, thus amplifying positive and negative scores.

In our algorithm, we employ a *Probability Proportional to Size* (PPS) sampling scheme that samples each element with probability proportional to a “size” measure. The use of PPS sampling has been pioneered in the context of distance query processing and successfully applied to computing closeness centralities in graphs [10]. In the context of clustering, PPS has been used to obtain samples whose clustering cost approximates the clustering cost of the whole dataset, with guarantees on the quality of the approximation [11]. To the best of our knowledge, prior to our work, the use of PPS for efficient clustering evaluation had not been explored.

## 1.2 Our Contributions

In this work, we target the problem of the efficient computation of an accurate estimate of the silhouette of a given clustering under general metric distances. In this regard, our contributions are:

- We develop the first efficient, sampling-based algorithm for estimating the silhouette with provable approximation guarantees. For any fixed  $\varepsilon, \delta \in (0, 1)$ , our algorithm approximates the silhouette of a  $k$ -clustering of  $n$  elements within an additive error  $4\varepsilon/(1-\varepsilon)$  with probability at least  $1-\delta$ , using only  $O(nk\varepsilon^{-2} \log(nk/\delta))$  distance computations, which constitutes a dramatic improvement over the  $\Theta(n^2)$  distance computations required by the naïve exact algorithm.
- We provide a distributed implementation of our algorithm using the Map-Reduce framework [12, 27], which runs in constant rounds, and requires only sublinear space at each worker.

<sup>1</sup><https://spark.apache.org/>

- We perform an extensive suite of experiments on real and synthetic datasets to assess the effectiveness and efficiency of our algorithm, and to compare it with known approaches for fast silhouette computation/approximation. The experiments show that, in practice, our algorithm provides silhouette estimates featuring very low absolute error (less than 0.01 in most cases) with small variance ( $< 10^{-3}$ ) using a very small fraction of the distance computations required by the exact calculation. Moreover, the estimates returned by our algorithm are far superior in quality to those returned by a naïve yet natural heuristics based on uniform sampling, or by the simplified silhouette [19] under general distances. We also show that the MapReduce implementation of our algorithm enables the estimation of the silhouette for clusterings of massive datasets (e.g., 1 billion elements) for which the exact computation is out of reach.

Our algorithm addresses the problematic issues posed by existing approaches by providing an efficiently computable and provably accurate approximation of the silhouette, allowing the use of the silhouette coefficient for very large datasets, for which its exact computation is unfeasible, and without the need to recur to other efficiently computable surrogates (such as the simplified silhouette coefficient) which in many cases provide estimates so divergent from the exact silhouette that they may lead to very different conclusions in the aforementioned scenarios of application.

In addition, while previously known approaches to efficiently compute or approximate the silhouette have been developed for specific distance functions, namely squared Euclidean and cosine distances, our algorithm provides provably accurate silhouette estimations for clusterings based on *any* metric distance. Finally, our algorithm can be generalized to compute rigorous approximations of other internal measures, such as cohesion and separation.

### 1.3 Organization of the paper

The rest of the paper is structured as follows. Section 2 contains the description of our proposed strategy for silhouette estimation, its accuracy and performance analysis, and the MapReduce implementation. Section 3 reports the results of an extensive suite of experiments performed to evaluate the effectiveness and scalability of our silhouette estimation algorithm on synthetic and real datasets. Section 4 concludes the paper with some final remarks.

## 2 Methods

Consider a metric space  $U$  with distance function  $d(\cdot, \cdot)$ , and let  $V = \{e_1, \dots, e_n\} \subseteq U$  be a dataset of  $n$  elements. Let also  $\mathcal{C} = \{C_1, \dots, C_k\}$  be a  $k$ -clustering of  $V$ , that is, a partition of  $V$  into  $k$  disjoint non-empty subsets called *clusters*. A popular measure to assess clustering quality was introduced by Rousseeuw in 1987 [28]. Specifically, the *silhouette of an element*  $e \in V$  belonging to some cluster  $C$ , is defined as

$$s(e) = \frac{b(e) - a(e)}{\max\{a(e), b(e)\}},$$

where

$$a(e) = \frac{\sum_{e' \in C} d(e, e')}{|C| - 1}, \quad b(e) = \min_{C_j \neq C} \frac{\sum_{e' \in C_j} d(e, e')}{|C_j|}$$

denote, respectively, the average distance of  $e$  from the other elements in its cluster, and the minimum average distance of  $e$  from the elements in some other cluster. The *silhouette of the clustering*  $\mathcal{C}$  is the average silhouette of all the elements of  $V$ , namely:

$$s(\mathcal{C}) = \frac{\sum_{i=1}^n s(e_i)}{n}. \quad (1)$$

From the above definitions it immediately follows that the values  $s(e)$ , with  $e \in V$ , and  $s(\mathcal{C})$  range in  $[-1, 1]$ . A positive value for  $s(e)$  implies that  $e$  has been assigned to an appropriate cluster, while a negative value implies that there might be a better cluster where  $e$  could have been placed. Therefore,  $s(e)$  can be interpreted as a measure of the quality of the clustering from the perspective of element  $e$ . In turn,  $s(\mathcal{C})$  provides a global measure of the quality of the whole clustering, where a value closer to 1 indicates higher quality. The exact computation of  $s(\mathcal{C})$  requires  $O(n^2)$  distance calculations, which is prohibitive when dealing with large datasets. In the following subsection, we present a randomized strategy to yield an estimate of  $s(\mathcal{C})$ , which is accurate within a provable error bound, with sufficiently high probability, and amenable to an efficient distributed computation.

## 2.1 A Fast Algorithm for Silhouette Estimation

Consider the estimation of the silhouette  $s(\mathcal{C})$  for a  $k$ -clustering  $\mathcal{C} = \{C_1, \dots, C_k\}$  of a set  $V$  of  $n$  elements from a metric space  $U$ . For each  $e \in V$  and  $C_j \in \mathcal{C}$ , define

$$W_{C_j}(e) = \sum_{e' \in C_j} d(e, e').$$

Note that for an element  $e$  of a cluster  $C$ , the quantities  $a(e)$  and  $b(e)$  in the definition of the silhouette  $s(e)$  can be rewritten as  $a(e) = W_C(e)/(|C| - 1)$  and  $b(e) = \min_{C_j \neq C} \{W_{C_j}(e_i)/|C_j|\}$ . Building on this observation, our approach to approximating  $s(\mathcal{C})$  is based on estimating the  $W_{C_j}(e)$ 's by exploiting the *Probability Proportional to Size* (PPS) sampling strategy used in [10]. In particular, for each cluster  $C_j \in \mathcal{C}$ , a suitable small sample  $S_{C_j}$  is computed, and, for every element  $e$ , the value of  $W_{C_j}(e)$  is approximated in terms of the distances between  $e$  and the elements of  $S_{C_j}$ , ensuring a user-defined error bound with high probability. The elements of  $S_{C_j}$  are chosen according to a carefully designed probability distribution which privileges the selection of elements that are distant from some suitable ‘‘central’’ element of the cluster. The details are given in what follows.

Consider a fixed error tolerance threshold  $0 < \varepsilon < 1$  and a probability  $0 < \delta < 1$ . Our algorithm, dubbed PPS-SILHOUETTE, consists of two *steps*. In Step 1, for each cluster  $C_j \in \mathcal{C}$ , the algorithm computes a sample  $S_{C_j}$  of expected size  $t = \lceil (c/2\varepsilon^2) \ln(4nk/\delta) \rceil$  for a suitably chosen constant  $c$ , while in Step 2 the approximate values of the  $W_{C_j}(e)$ 's and, in turn, the approximations of the  $s(e)$ 's are computed through the  $S_{C_j}$ 's. More precisely, in Step 1, each cluster  $C_j$  is processed independently. If  $|C_j| \leq t$ , then  $S_{C_j}$  is set to  $C_j$ , otherwise, *Poisson sampling* is performed over  $C_j$ , that is, each element  $e \in C_j$  is included in  $S_{C_j}$  independently with a suitable probability  $p_e$ . Probability  $p_e$ , for  $e \in C_j$ , is determined as follows:

- First, an initial sample  $S_{C_j}^{(0)}$  is selected, again by Poisson sampling, where each  $e \in C_j$  is included in  $S_{C_j}^{(0)}$  independently with probability  $(2/|C_j|) \ln(2k/\delta)$ . This initial sample will contain, with sufficiently high probability, the aforementioned ‘‘central’’ element of  $C_j$ , namely, one that is close to a majority of the elements of  $C_j$ , a property which is necessary to enforce the quality of the final sample  $S_{C_j}$ ;
- For each  $\bar{e} \in S_{C_j}^{(0)}$  the value  $W_{C_j}(\bar{e})$  is computed, and, for each  $e \in C_j$ ,  $p_e$  is set to  $\min\{1, t\gamma_e\}$ , where  $\gamma_e$  is the maximum between  $1/|C_j|$  (corresponding to uniform sampling) and the maximum of the values  $d(e, \bar{e})/W_{C_j}(\bar{e})$ , with  $\bar{e} \in S_{C_j}^{(0)}$  (representing the relative contributions of  $e$  to the  $W_{C_j}(\bar{e})$ 's of the sample points).

In Step 2, for each  $e \in V$  and each cluster  $C_j$ , the sample  $S_{C_j}$  is used to compute the value

$$\hat{W}_{C_j}(e) = \sum_{e' \in S_{C_j}} \frac{d(e, e')}{p_{e'}}$$

which is an accurate estimator of  $W_{C_j}(e)$ , as will be shown by the analysis. Once all these values have been computed, then, for each  $e \in V$  belonging to a cluster  $C$  we compute the estimates  $\hat{a}(e) = \hat{W}_C(e)/(|C| - 1)$  and  $\hat{b}(e) = \min_{C_j \neq C} \{\hat{W}_{C_j}(e)/|C_j|\}$ , which are in turn used to estimate the silhouette as  $\hat{s}(e) = (\hat{b}(e) - \hat{a}(e))/(\max\{\hat{a}(e), \hat{b}(e)\})$ . Finally, we estimate the silhouette of the whole clustering as

$$\hat{s}(\mathcal{C}) = \frac{\sum_{e \in V} \hat{s}(e)}{n}. \quad (2)$$

## 2.2 Analysis

In this section we show that, with probability  $1 - \delta$ , the value  $\hat{s}(\mathcal{C})$  computed by PPS-SILHOUETTE approximates the true silhouette  $s(\mathcal{C})$  within a small error bound, expressed in terms of  $\varepsilon$ . The key ingredient towards this goal, stated in the following theorem, is a probabilistic upper bound on the relative error of the estimate  $\hat{W}_{C_j}(e)$  with respect to true value  $W_{C_j}(e)$ .

**Theorem 1.** *There is a suitable choice of the constant  $c$  in the definition of the expected sample size  $t$  used by PPS-SILHOUETTE, which ensures that, with probability at least  $1 - \delta$ , for every element  $e$  and every cluster  $C_j$ , the estimate  $\hat{W}_{C_j}(e)$  is such that*

$$\left| \frac{\hat{W}_{C_j}(e) - W_{C_j}(e)}{W_{C_j}(e)} \right| \leq \varepsilon.$$

---

**Algorithm 1:** PPS-SILHOUETTE( $V, \mathcal{C}, \varepsilon, \delta$ )

**Input:** clustering  $\mathcal{C} = \{C_1, \dots, C_k\}$  of  $V$ ,  $\varepsilon, \delta \in (0, 1)$ 
**Output:** estimate  $\hat{s}(\mathcal{C})$  of  $s(\mathcal{C})$ .

// Step 1: PPS sampling

 $n \leftarrow |V|;$ 
 $t \leftarrow \lceil \frac{c}{2\varepsilon^2} \ln(4nk/\delta) \rceil;$  // (expected sample size)

**for each** cluster  $C_j \in \mathcal{C}$  **do**

     **if**  $t \geq |C_j|$  **then**  $S_{C_j} \leftarrow C_j;$ 

     **else**

          $S_{C_j}^{(0)} \leftarrow$  Poisson sampling of  $C_j$  with probability  
                  $(2/|C_j|) \ln(2k/\delta);$ 

         **for each**  $\bar{e} \in S_{C_j}^{(0)}$  **do**  $W_{C_j}(\bar{e}) \leftarrow \sum_{e' \in C_j} d(\bar{e}, e');$ 

         **for each**  $e \in C_j$  **do**

              $\gamma_e \leftarrow \max\{d(e, \bar{e})/W_{C_j}(\bar{e}) : \bar{e} \in S_{C_j}^{(0)}\};$ 

              $\gamma_e \leftarrow \max\{\gamma_e, 1/|C_j|\};$ 

              $p_e \leftarrow \min\{1, t\gamma_e\};$ 

         **end**

          $S_{C_j} \leftarrow$  Poisson sampling of  $C_j$  with probabilities  
                  $\{p_e : e \in C_j\};$ 

     **end**
**end**

// Step 2: silhouette estimation

**for each**  $e \in V$  **do**

     Let  $e$  belong to cluster  $C;$ 

     **for each** cluster  $C_j$  **do**

          $\hat{W}_{C_j}(e) = \sum_{e' \in S_{C_j}} d(e, e')/p_{e'};$ 

     **end**

      $\hat{a}(e) \leftarrow \hat{W}_C(e)/(|C| - 1);$ 

      $\hat{b}(e) \leftarrow \min\{\hat{W}_{C_j}(e)/|C_j| : C_j \neq C\};$ 

      $\hat{s}(e) \leftarrow (\hat{b}(e) - \hat{a}(e))/(\max\{\hat{a}(e), \hat{b}(e)\});$ 
**end**
 $\hat{s}(\mathcal{C}) \leftarrow \sum_{e \in V} \hat{s}(e)/n;$ 
**return**  $\hat{s}(\mathcal{C})$ 


---

*Proof.* The proof mimics the argument devised in [10]. Recall that  $t = \lceil \frac{c}{2\varepsilon^2} \ln(4nk/\delta) \rceil$ . Consider an arbitrary cluster  $C_j$  with more than  $t$  elements (in the case  $|C_j| \leq t$  the theorem follows trivially). For an element  $e \in C_j$ , let  $m(e)$  denote the median of the distances from  $e$  to all other elements of  $C_j$ . Element  $e$  is called *well positioned* if  $m(e) \leq 2 \min_{e' \in C_j} m(e')$ . It is easy to see that at least half of the elements of  $C_j$  are well positioned. Hence, the initial random sample  $S_{C_j}^{(0)}$  will contain a well positioned element with probability at least  $(1 - (2/|C_j|) \ln(2k/\delta))^{|C_j|/2} \geq 1 - \delta/(2k)$ . An easy adaptation of the proof of [10, Lemma 12], shows that if  $S_{C_j}^{(0)}$  contains a well positioned element and  $c$  is a suitable constant, then the Possion sample  $S_{C_j}$  computed with the probabilities derived from  $S_{C_j}^{(0)}$  is such that  $|(\hat{W}_{C_j}(e) - W_{C_j}(e))/W_{C_j}(e)| \leq \varepsilon$ , with probability at least  $1 - \delta/(2nk)$ . By the union bound, it follows that the probability that there exists a cluster  $C_j$  such that the initial sample  $S_{C_j}^{(0)}$  does not contain a well positioned element is at most  $k\delta/(2k) = \delta/2$ . Also, by conditioning on the fact that for all clusters  $C_j$  the initial sample  $S_{C_j}^{(0)}$  contains a well positioned node, by using again the union bound we obtain that the probability that there exists an element  $e$  and a cluster  $C_j$  for which  $|(\hat{W}_{C_j}(e) - W_{C_j}(e))/W_{C_j}(e)| > \varepsilon$  is at most  $nk\delta/(2nk) = \delta/2$ , which concludes the proof.  $\square$

From now on, we assume that the relative error bound stated in Theorem 1 holds for every element  $e \in V$  and every cluster  $C_j$ , an event which we will refer to as *event E*. Consider an arbitrary element  $e$ , and let  $\hat{s}(e)$  be the estimate of the silhouette  $s(e)$  computed by PPS-SILHOUETTE. The following key technical lemma, establishes a bound on the absolute error of the estimate.

**Lemma 1.** *If event  $E$  holds, then  $|\hat{s}(e) - s(e)| \leq 4\varepsilon/(1 - \varepsilon)$ .*

*Proof.* We first show that, if event  $E$  holds, the relative errors  $|(\hat{a}(e) - a(e))/a(e)|$  and  $|(\hat{b}(e) - b(e))/b(e)|$  are both upper bounded by  $\varepsilon$ . For what concerns the former error, the bound follows immediately from the definition of  $\hat{a}(e)$  and the relative error bound assumed for  $\hat{W}_{C_j}(e)$ . For the latter, consider an arbitrary cluster  $C_j$  and let  $b_{C_j}(e) = W_{C_j}(e)/|C_j|$  and  $\hat{b}_{C_j}(e) = \hat{W}_{C_j}(e)/|C_j|$ . Arguing as for the previous bound, we can easily show that  $|(\hat{b}_{C_j}(e) - b_{C_j}(e))/b_{C_j}(e)| \leq \varepsilon$ . Recall that  $b(e) = \min_{C_j \neq C} b_{C_j}(e)$  and that  $\hat{b}(e) = \min_{C_j \neq C} \hat{b}_{C_j}(e)$ . Suppose that  $b(e) = b_{C'}(e)$  and  $\hat{b}(e) = \hat{b}_{C''}(e)$ , for some, possibly different, clusters  $C'$  and  $C''$ . We have:

$$(1 - \varepsilon)b(e) = (1 - \varepsilon)b_{C'}(e) \leq (1 - \varepsilon)b_{C''}(e) \leq \hat{b}_{C''}(e) = \hat{b}(e)$$

and

$$\hat{b}(e) = \hat{b}_{C''}(e) \leq \hat{b}_{C'}(e) \leq (1 + \varepsilon)b_{C'}(e) = (1 + \varepsilon)b(e),$$

and the desired bound follows.

Now we establish a bound on the relative error for the term appearing in the denominator of the formula defining  $\hat{s}(e)$ . Define  $m(e) = \max\{a(e), b(e)\}$  and  $\hat{m}(e) = \max\{\hat{a}(e), \hat{b}(e)\}$ . We show that  $|(\hat{m}(e) - m(e))/m(e)| \leq \varepsilon$ . Suppose that  $m(e) = a(e)$ , hence  $a(e) \geq b(e)$  (the case  $m(e) = b(e)$  can be dealt with similarly). If  $\hat{m}(e) = \hat{a}(e)$ , the bound is immediate. Instead, if  $\hat{m}(e) = \hat{b}(e)$ , hence  $\hat{b}(e) \geq \hat{a}(e)$ , the bound follows since

$$\begin{aligned} \hat{m}(e) = \hat{b}(e) &\leq (1 + \varepsilon)b(e) \\ &\leq (1 + \varepsilon)a(e) = (1 + \varepsilon)m(e), \end{aligned}$$

and

$$\begin{aligned} \hat{m}(e) = \hat{b}(e) &\geq \hat{a}(e) \\ &\geq (1 - \varepsilon)a(e) \\ &= (1 - \varepsilon)m(e). \end{aligned}$$

We are now ready to derive the desired bound on  $|\hat{s}(e) - s(e)|$ . By virtue of the relative error bounds established above, we have that

$$\hat{s}(e) = \frac{\hat{b}(e) - \hat{a}(e)}{\hat{m}(e)} \leq \frac{(1 + \varepsilon)b(e) - (1 - \varepsilon)a(e)}{(1 - \varepsilon)m(e)}.$$

Straightforward transformations show that

$$\frac{(1 + \varepsilon)b(e) - (1 - \varepsilon)a(e)}{(1 - \varepsilon)m(e)} = s(e) + \frac{2\varepsilon}{1 - \varepsilon} \left( s(e) + \frac{a(e)}{m(e)} \right)$$

Since  $s(e) \leq 1$  and  $a(e) \leq m(e)$ , we get

$$\hat{s}(e) \leq s(e) + \frac{4\varepsilon}{1 - \varepsilon}.$$

In a similar fashion, it follows that

$$\begin{aligned} \hat{s}(e) &= \frac{\hat{b}(e) - \hat{a}(e)}{\hat{m}(e)} \\ &\geq \frac{(1 - \varepsilon)b(e) - (1 + \varepsilon)a(e)}{(1 + \varepsilon)m(e)} \\ &= s(e) - \frac{2\varepsilon}{1 + \varepsilon} \left( s(e) + \frac{a(e)}{m(e)} \right) \\ &\geq s(e) - \frac{4\varepsilon}{1 + \varepsilon} \geq s(e) - \frac{4\varepsilon}{1 - \varepsilon}. \end{aligned}$$

□

An upper bound to the absolute error incurred when estimating  $s(C)$  through the value  $\hat{s}(C)$  computed by PPS-SILHOUETTE, is established in the following theorem, whose proof is an immediate consequence of the definition of the two quantities (Equations 1 and 2), and of Theorem 1 and Lemma 1.

**Theorem 2.** *Let  $V$  be a dataset of  $n$  elements, and let  $\mathcal{C}$  be a  $k$ -clustering of  $V$ . Let  $\hat{s}(\mathcal{C})$  be the estimate of the silhouette of the clustering  $s(\mathcal{C})$  computed by PPS-SILHOUETTE for given parameters  $\varepsilon$  and  $\delta$ , with  $0 < \varepsilon, \delta < 1$ , and for a suitable choice of constant  $c > 0$  in the definition of the sample size. Then,*

$$|\hat{s}(\mathcal{C}) - s(\mathcal{C})| \leq \frac{4\varepsilon}{1 - \varepsilon}$$

with probability at least  $1 - \delta$ .

We now analyze the running time of PPS-SILHOUETTE, assuming that the distance between two points can be computed in constant time. In Step 1, the running time is dominated by the computation of the distances between the points of each sufficiently large cluster  $C_j$  and the points that form the initial sample  $S_{C_j}^{(0)}$ . A simple application of the Chernoff bound shows that, with high probability, from each such cluster  $C_j$ ,  $O(\log(nk/\delta))$  points are included in  $S_0^j$ . Thus, Step 1 performs  $O(n \log(nk/\delta))$  distance computations, altogether. For what concerns Step 2, its running time is dominated by the computation of the distances between all points of  $V$  and the points of the union of all samples. A simple adaptation of the proof of [10, Corollary 11] and a straightforward application of the Chernoff bound shows that there are  $O(kt)$  sample points overall, with high probability, where  $t$  is the expected sample size for each cluster. Recalling that  $t = \lceil (c/2\varepsilon^2) \ln(4nk/\delta) \rceil$ , we have that Step 2 performs  $O(nkt) = O((nk\varepsilon^{-2}) \log(nk/\delta))$  distance computations overall. As a consequence, the running time of the algorithm is  $O(nk\varepsilon^{-2} \log(nk/\delta))$  which, for reasonable values of  $k$ ,  $\varepsilon$  and  $\delta$ , is a substantial improvement compared to the quadratic complexity of the exact computation.

We remark that while the  $\varepsilon^{-2}$  factor in the upper bound on the sample size might result in very large samples to achieve high accuracy, this quadratic dependence on  $\varepsilon$  reflects a worst-case scenario and is needed to obtain the analytical bound. In fact, Section 3 will provide experimental evidence that, in practice, rather modest sample sizes are sufficient to achieve high levels of accuracy.

### 2.3 Generalization To Other Measures

The PPS-based sampling strategy adopted for approximating the silhouette of a clustering can be applied to other measures used for internal clustering evaluation, which are based on sums of distances between points of the dataset. This is the case, for instance, of measures that compare the *cohesion* (i.e., the average intracluster distance) and the *separation* (i.e., the average intercluster distance) of the clustering [30].

More precisely, consider a  $k$ -clustering  $\mathcal{C} = \{C_1, \dots, C_k\}$  and define the cohesion and separation of  $\mathcal{C}$  as

$$\begin{aligned} \text{Coh}(\mathcal{C}) &= \frac{1}{2} \frac{\sum_{j=1}^k \sum_{e', e'' \in C_j} d(e', e'')}{\sum_{j=1}^k \binom{|C_j|}{2}} \\ \text{Sep}(\mathcal{C}) &= \frac{\sum_{1 \leq j_1 < j_2 \leq k} \sum_{e' \in C_{j_1}} \sum_{e'' \in C_{j_2}} d(e', e'')}{\sum_{1 \leq j_1 < j_2 \leq k} (|C_{j_1}| |C_{j_2}|)}, \end{aligned}$$

respectively. (These measures have been also employed to assess the average cluster reliability for a clustering of a network where distances correspond to connection probabilities [8, 31].) We can rewrite the above measures in terms of the sums  $W_C(e)$  defined in the previous section, as follows

$$\begin{aligned} \text{Coh}(\mathcal{C}) &= \frac{1}{2} \frac{\sum_{j=1}^k \sum_{e \in C_j} W_{C_j}(e)}{\sum_{j=1}^k \binom{|C_j|}{2}} \\ \text{Sep}(\mathcal{C}) &= \frac{\sum_{1 \leq j_1 < j_2 \leq k} \sum_{e \in C_{j_1}} W_{C_{j_2}}(e)}{\sum_{1 \leq j_1 < j_2 \leq k} (|C_{j_1}| |C_{j_2}|)} \end{aligned}$$

Clearly, approximations of the  $W_C(e)$ 's with low relative errors immediately yield approximations with low relative error for  $\text{Coh}(\mathcal{C})$  and  $\text{Sep}(\mathcal{C})$ . Specifically, define  $\widehat{\text{Coh}}(\mathcal{C})$  and  $\widehat{\text{Sep}}(\mathcal{C})$  as the respective approximations to  $\text{Coh}(\mathcal{C})$  and  $\text{Sep}(\mathcal{C})$  obtained by substituting each  $W_C(e)$  occurring in the above equations with the value  $\hat{W}_C(e)$  computed within PPS-SILHOUETTE. The following theorem is an immediate consequence of Theorem 2.1.

**Theorem 3.** *Let  $V$  be a dataset of  $n$  elements, and let  $\mathcal{C}$  be a  $k$ -clustering of  $V$ . Let  $\widehat{\text{Coh}}(\mathcal{C})$  and  $\widehat{\text{Sep}}(\mathcal{C})$  be the respective approximations to  $\text{Coh}(\mathcal{C})$  and  $\text{Sep}(\mathcal{C})$  based on the values  $\hat{W}_C(e)$  computed within PPS-SILHOUETTE for*

given parameters  $\varepsilon$  and  $\delta$ , with  $0 < \varepsilon, \delta < 1$ , and for a suitable choice of constant  $c > 0$  in the definition of the sample size. Then,

$$\left| \frac{\widehat{\text{Coh}}(\mathcal{C}) - \text{Coh}(\mathcal{C})}{\text{Coh}(\mathcal{C})} \right| \leq \varepsilon$$

$$\left| \frac{\widehat{\text{Sep}}(\mathcal{C}) - \text{Sep}(\mathcal{C})}{\text{Sep}(\mathcal{C})} \right| \leq \varepsilon$$

with probability at least  $1 - \delta$ .

## 2.4 Map-Reduce Implementation

Throughout the algorithm, a key-value pair will be written as  $(key \mid value_1, \dots, value_r)$ , where  $\langle value_1, \dots, value_r \rangle$  is an  $r$ -dimensional value. Consider a  $k$ -clustering  $\mathcal{C} = \{C_1, \dots, C_k\}$  of a dataset  $V = \{e_1, \dots, e_n\}$  of  $n$  elements. We assume that, initially, the clustering is represented by the following set of key-value pairs:

$$\{(i|e_i, j_i) : 1 \leq i \leq n \wedge e_i \in C_{j_i}\}.$$

We also assume that the values  $n, k, t$  used in PPS-SILHOUETTE, as well as all  $|C_j|$ 's, are given to the program. Recall that our implementation, outlined in the main paper, partitions the points of  $V$  into  $w$  subsets of size  $n/w$  each, where  $w \in [0, n - 1]$  is a suitable design parameter. The four rounds are described in detail below. As customary in the description of MapReduce algorithms, we will use the term *reducer* to refer to the application of a reduce function to a set of pairs with same key.

### Round 1:

- **Map:** Map each pair  $(i|e_i, j_i)$  into the pair  $(i \bmod w|e_i, j_i, 0)$ . Also, with probability  $(2/|C_{j_i}|) \ln(2k/\delta)$  select  $e_i$  to be part of the initial Poisson sample  $S_{C_{j_i}}^{(0)}$ , and produce the  $w$  additional pairs  $(\ell|e_i, j_i, 1)$ , with  $0 \leq \ell < w$ .
- **Reduce:** Let  $V_\ell$  be the set of elements  $e_i$  for which there is a pair  $(\ell|e_i, j_i, 0)$ . (Observe that the  $V_\ell$ 's form a balanced partition of  $V$  into  $w$  subsets.) For each pair  $(\ell|e_i, j_i, 1)$  compute the sum  $W_{i,\ell}$  of the distances from  $e_i$  to all elements of  $V_\ell \cap C_{j_i}$  and produce the pair  $(\ell|e_i, j_i, W_{i,\ell}, 1)$ . Instead, for each pair  $(\ell|e_i, j_i, 0)$  produce the pair  $(\ell|e_i, j_i, 0, 0)$ .

By the analysis (see main paper), we know that, with high probability,  $O(k \ln(nk/\delta))$  points have been selected to be part of the initial samples  $S_{C_{j_i}}^{(0)}$ 's (a copy of all these points, represented by pairs with 1 at the end, exists for each key  $\ell$ ). Therefore, this round requires local memory  $M_L = O(n/w + k \ln(nk/\delta))$ , with high probability, and aggregate memory  $M_A = O(wM_L)$ .

### Round 2:

- **Map:** Map each pair  $(\ell|e_i, j_i, 0, 0)$  into itself, and each pair  $(\ell|e_i, j_i, W_{i,\ell}, 1)$  into the  $w$  pairs  $(\ell'|e_i, j_i, W_{i,\ell}, 1)$ , with  $0 \leq \ell' < w$ .
- **Reduce:** Each reducer, corresponding to some key  $\ell$ , now contains all the information needed to compute the values  $W_C(e)$  for each cluster  $C$  and element  $e \in S_C^{(0)}$ . This in turn implies that the reducer can also compute all sampling probabilities  $p(e_i)$  for  $e_i \in V_\ell$ , by executing the operations specified in PPS-SILHOUETTE. The reducer computes these probabilities and produces the pairs  $(\ell|e_i, j_i, p(e_i))$ , one for each  $e_i \in V_\ell$ .

By the observations made at the end of Round 1, this round requires local memory  $M_L = O(n/w + wk \log(nk/\delta))$ , with high probability, and aggregate memory  $M_A = O(wM_L)$ .

### Round 3:

- **Map:** Map each pair  $(\ell|e_i, j_i, p(e_i))$  into the pair  $(\ell|e_i, j_i, 0)$ . Also, with probability  $p(e_i)$  select  $e_i$  to be part of the Poisson sample  $S_{C_{j_i}}$ , and produce the  $w$  additional pairs  $(\ell'|e_i, j_i, 1)$ , with  $0 \leq \ell' < w$ .

- **Reduce Phase:** Each reducer, corresponding to some key  $\ell$ , now contains all the information needed to compute the approximate silhouette values  $\hat{s}(e_i)$  for each element in  $e_i \in V_\ell$  and then sum them into  $\hat{s}_\ell$ , producing the single pair  $(0|\hat{s}_\ell)$ .

By the analysis (see main paper), we know that, with high probability, the size of union of the Poisson samples  $S_{C_j}$ 's is  $O(kt)$ , with  $t = \lceil c/(2\varepsilon^2) \ln(4nk/\delta) \rceil$ . Therefore, this round requires local memory  $M_L = O(n/w + kt) = O(n/w + (k/\varepsilon^2) \log(nk/\delta))$ , with high probability, and aggregate memory  $M_A = O(wM_L)$ .

#### Round 4:

- **Map:** identity map.
- **Reduce:** The reducer corresponding to key 0 computes and returns  $\hat{s}_C = (1/n) \sum_{\ell=0}^{w-1} \hat{s}_\ell$ .

This round requires  $M_L = M_A = O(w)$ .

Overall, the above 4-round MapReduce algorithm requires local memory  $M_L = O(n/w + (w + 1/\varepsilon^2)k \log(nk/\delta))$ , with high probability, and aggregate memory  $M_A = O(wM_L)$ .

### 3 Experimental Evaluation

We ran extensive experiments with the twofold objective of assessing the quality and evaluating the performance of our PPS-SILHOUETTE algorithm. Concerning quality assessment, we evaluate the accuracy of the estimate provided by PPS-SILHOUETTE, and compare it against known heuristic and exact (specialized) baselines. For what concerns performance, we evaluate the scalability of the MapReduce implementation of PPS-SILHOUETTE and compare its performance against the one of the aforementioned baselines.

#### 3.1 Baselines

We gauge the performance of our PPS-SILHOUETTE algorithm against five *baselines*. The first baseline is the exact computation based on the definition. The second baseline is a variation of PPS-SILHOUETTE, where the samples  $S_{C_j}$  are chosen via a uniform Poisson sampling, using the same probability  $p(e) = t/|C_j|$  for each  $e \in C_j$ . The other three baselines implement, respectively, the simplified silhouette of [19, 33], the Frahling-Sohler optimization of the exact computation [15], and the optimized exact method available in the Apache Spark library for squared Euclidean distances (see Section 1.1) Our quality assessment compares PPS-SILHOUETTE against the approximation baselines, namely uniform sampling and simplified silhouette, while our performance evaluation compares PPS-SILHOUETTE against all baselines except for simplified silhouette, since the latter turned out to have low accuracy.

#### 3.2 Implementation and Environment

For quality assessment, we devised Java-based sequential implementations of PPS-SILHOUETTE, of the exact computation, based on the definition, and of the uniform sampling and simplified silhouette baselines. For performance evaluation, we devised MapReduce implementations, using the Apache Spark programming framework with Java<sup>2</sup>, of all baselines except simplified silhouette and the Apache Spark optimized method, whose code is provided in the Spark library. The MapReduce implementation of the uniform sampling baseline is patterned after the one of PPS-SILHOUETTE, by only changing the sampling probabilities. The MapReduce implementation of the exact silhouette computation aims at minimizing the computational load per worker by evenly partitioning the operations among the workers and by providing each worker with an entire copy of the dataset. Finally, the MapReduce implementation of the Frahling-Sohler optimization enforces the optimistic scenario where the heuristics for the  $b(e)$  term, in the computation of  $s(e)$ , is always successful, in order to appreciate the maximum speed-up that can be achieved over the non-optimized implementation<sup>3</sup>.

In our experiments we fixed  $\delta = 0.1$ , resulting in a 90% confidence on the approximation guarantee, and we opted to control accuracy by varying the composite parameter  $t$  directly rather than fixing the independent variables  $\varepsilon$  and  $c$  separately (see Section 2.2).

<sup>2</sup><https://spark.apache.org>

<sup>3</sup>All our implementations are available at <https://github.com/CalebTheGame/AppxSilhouette>

The experiments were run on CloudVeneto<sup>4</sup>, an institutional cloud, which provided us a cluster of 9 PowerEdge M620 nodes, each with octa-core Intel Xeon E5-2670v2 2.50 GHz and 16 GB of RAM, running Ubuntu 16.04.3 LTS with Hadoop 2.7.4 and Apache Spark 2.4.4.

Table 1: Maximum and average absolute error of the silhouette estimates returned by PPS-SILHOUETTE (label “PPS”) and the uniform sampling algorithm, (label “uniform”) relative to the  $k$ -medoid clustering of the synthetic dataset with  $n = 2 \cdot 10^4$  points,  $k = 2, 3 \dots, 10$ , and  $t = 64, 256$  and  $1024$ , alongside with absolute error of the simplified silhouette. Values  $< 10^{-3}$  are denoted by  $0^*$ .

k	Absolute Error												
	Simplified silhouette	PPS						Uniform					
		t=64		t=256		t=1024		t=64		t=256		t=1024	
		max	avg	max	avg	max	avg	max	avg	max	avg	max	avg
2	.283	.005	.001	.002	0*	.001	0*	.207	.145	.206	.143	.199	.116
3	.404	.018	.005	.008	.002	.004	.001	.369	.235	.403	.217	.392	.163
4	.026	.012	.003	.005	.001	.002	0*	.492	.291	.473	.301	.458	.150
5	.561	.015	.005	.008	.002	.004	.001	.174	.404	.487	.322	.438	.159
6	.314	.101	.015	.034	.007	.010	.002	.174	.082	.126	.049	.052	.005
7	.449	.047	.010	.016	.004	.010	.002	.280	.174	.273	.121	.097	.025
8	.321	.084	.017	.028	.006	.008	.002	.168	.075	.149	.349	.013	.002
9	.455	.078	.013	.015	.003	.003	0*	.295	.187	.254	.188	.068	.002
10	.457	.050	.013	.013	.003	.003	0*	.284	.180	.246	.108	.071	.002

### 3.3 Datasets

We considered both synthetic and real datasets. Synthetic datasets have been chosen so to contain a few outlier points, with the intent of making the accurate estimation of the silhouette more challenging. Specifically, for different values of  $n$  (ranging from tens of thousands to one billion), we generated  $n - 10$  points uniformly at random within the sphere of unit radius, centered at the origin of the 3-dimensional Euclidean space, and 10 random points on the surface of the concentric sphere of radius  $10^4$ . For real datasets, we used reduced versions of the “Coverttype” and “HIGGS” datasets<sup>5</sup>. The former contains 100000 55-dimensional points, corresponding to tree observations from four areas of the Roosevelt National Forest in Colorado; the latter contains 500000 7-dimensional points and is used to train learning algorithms for high-energy Physics experiments (as in previous works [9, 23], only the 7 summary attributes of the original 28 have been retained). For all datasets, the clusterings used to test the algorithms have been obtained by applying the  $k$ -medoids clustering algorithm implemented in the Java Machine Learning Library<sup>6</sup> [1], using the Euclidean distance.

### 3.4 Quality Assessment

In the first experiment, we compared the accuracy of the silhouette estimations returned by our PPS-SILHOUETTE algorithm and by the uniform sampling algorithm, using synthetic data. In order to make the computation of the exact value feasible, we considered instances of the synthetic dataset with a relatively small number of elements ( $n = 2 \times 10^4$ ) and  $k$ -clusterings  $\mathcal{C}$  with  $k \in \{2, \dots, 10\}$ . As explained in Section 3.2, the accuracy of PPS-SILHOUETTE, and, clearly, also of the uniform sampling algorithm, depends on the (expected) sample size  $t$ . Hence, to test different levels of accuracy, for each value of  $k$  we conveniently varied the value  $t$  directly. We remark that, in general, controlling the sample size  $t$  directly, rather than indirectly through the several parameters contributing to its definition, is more effective in practice since it affords a better tailoring of the estimation to the available resources. Specifically, we ran both PPS-SILHOUETTE and the uniform sampling algorithm with  $t \in \{64, 128, 256, 512, 1024\}$ . As a measure of accuracy for the estimated silhouette  $\hat{s}(\mathcal{C})$ , we use the absolute error  $|\hat{s}(\mathcal{C}) - s(\mathcal{C})|$ . Table 1 reports maximum and average of the absolute error over 100 runs of the two algorithms, for each configuration of parameters  $k$  and a selection of  $t$ 's (the results for the other values of  $t$ , omitted for brevity, are similar to the ones reported in the table).

The results show that PPS-SILHOUETTE provides a very accurate approximation to the silhouette already with  $t = 64$ , for which the average absolute error is at most 0.017 for all values of  $k$  and the maximum value is at most 0.084 for all cases but  $k = 6$ . The approximation quickly improves when larger values of  $t$  are considered. PPS-SILHOUETTE also

<sup>4</sup><http://cloudveneto.it>

<sup>5</sup><https://archive.ics.uci.edu/ml/datasets/>

<sup>6</sup><https://github.com/AbeelLab/javaml>

features a very low variance, which is  $< 10^{-3}$  in all cases. These results show that our PPS-SILHOUETTE algorithm provides a very accurate approximation of the silhouette even with a limited number of samples.

Table 2: Comparison between exact silhouette, simplified silhouette, and Monte Carlo estimates obtained by averaging 100 estimates returned by PPS-SILHOUETTE (label “PPS”) and the uniform sampling algorithm (label “uniform”), for  $k = 2, 3, \dots, 10$  and  $t = 64, 128$  and  $1024$ . The highest value identified by each algorithm (one for each  $t$  for PPS and uniform) is highlighted in boldface. Observe that the “correct” value of  $k$  corresponds to the value with highest exact silhouette.

k			Silhouette					
			PPS			uniform		
			Exact	Simplified	t=64	t=256	t=1024	t=64
2	0.064	0.347	0.064	0.064	0.064	<b>0.192</b>	<b>0.176</b>	0.074
3	-0.072	0.332	-0.070	-0.072	-0.072	0.151	0.081	-0.191
4	<b>0.343</b>	0.369	<b>0.343</b>	<b>0.344</b>	<b>0.343</b>	0.049	0.039	<b>0.183</b>
5	-0.228	0.333	-0.223	-0.228	-0.226	0.158	0.031	-0.244
6	0.034	0.348	0.022	0.032	0.034	0.121	0.071	0.040
7	-0.143	0.306	-0.148	-0.145	-0.143	0.033	-0.030	-0.130
8	0.059	<b>0.380</b>	0.038	0.055	0.058	0.134	0.094	0.057
9	-0.087	0.368	-0.102	-0.091	-0.088	0.102	0.021	-0.087
10	-0.104	0.353	-0.116	-0.017	-0.104	0.073	0.005	-0.103

On the other hand, for  $t = 64$  the uniform sampling algorithm provides estimates with considerably larger average and maximum absolute errors for most values of  $k$ , with an average error that is one order of magnitude larger than the average error of PPS-SILHOUETTE. The variance of the uniform sampling algorithm (0.05 on average) is also larger than the one of our algorithm. These results show that the use of PPS sampling is crucial to obtain good estimates of the silhouette while keeping the sample size small.

The second column of Table 1 shows the error that occurs when the simplified silhouette is used to approximate the exact value of the silhouette. Such error is always larger than twice the maximum error provided by PPS-SILHOUETTE (even for the smallest values of the sample size  $t$ ) and is approximately 0.36 on average, which is not surprising considering the weak relation between simplified silhouette and the exact value of the silhouette quantified by [33]. Therefore, the simplified silhouette does not provide accurate estimates of the exact value of the silhouette.

Table 3: Comparison between exact silhouette, simplified silhouette, and maximum and average absolute error of the silhouette estimates returned by PPS-SILHOUETTE (label “PPS”) and the uniform sampling algorithm, (label “uniform”), relative to the  $k$ -medoid clustering of the real datasets Covertyp and HIGGS, with  $k = 5, 10$  and  $t = 64, 256$  and  $1024$ .

Dataset	k	Absolute error													
		Silhouette		PPS						Uniform					
				t = 64		t = 256		t = 1024		t = 64		t = 256		t = 1024	
Exact	Simpl.	max	avg	max	avg	max	avg	max	avg	max	avg	max	avg		
Covertyp	5	0.344	0.474	.084	.016	.042	.006	.007	.002	.108	.019	.027	.007	.014	.003
	10	0.266	0.394	.120	.023	.025	.006	.014	.002	.160	.031	.040	.009	.014	.002
HIGGS	5	0.244	0.368	.114	.016	.024	.006	.008	.003	.110	.017	.045	.008	.019	.003
	10	0.151	0.289	.107	.028	.047	.010	.020	.004	.155	.033	.081	.012	.019	.005

In the second experiment, we assessed the impact of relying on estimated rather than exact values in the most typical scenario of use of the silhouette, suggested in the original paper [28], that is, identifying the best granularity  $k$  when the same clustering algorithm is applied to a dataset with different values of  $k$ . Specifically, we ran  $k$ -medoids clustering on the synthetic dataset described above, for all values of  $k$  in an interval  $[2, 10]$ , and checked whether the best clustering (according to the exact silhouette) was identified using the silhouette estimations returned by PPS-SILHOUETTE and by the uniform sampling algorithm with expected sample size  $t$ , considering values of  $t \in \{64, 256, 1024\}$ . Since uniform sampling displays a large variance affecting its silhouette estimates, we adopted a Monte Carlo approach, where the average of 100 independent estimates is used in lieu of a single estimate, to reduce the variance of the estimates. We also computed the deterministic value of the simplified silhouette [19, 33] to compare its effectiveness against the two sampling strategies. The results are shown in Table 2, where the exact value of the silhouette is also shown.

As expected, PPS-SILHOUETTE always identifies the correct value already for  $t = 64$ , and, for all  $k$  and  $t$ , it provides extremely accurate approximations. On the other hand, the uniform sampling algorithm identifies the correct value of  $k$  only for  $t = 1024$ , and, for smaller values of  $t$ , it provides much weaker approximations (indeed,  $t = 512$  is needed merely to hit the correct sign of the silhouette value for all  $k$ ). Also, the table shows that the simplified silhouette is unable to identify the correct value of  $k$ .

Table 4: Identification of the value of  $k$  yielding the highest silhouette using PPS-SILHOUETTE (label “PPS”) and the uniform sampling algorithm (label “uniform”). For each range of  $k \in [2, \ell]$ , with  $\ell = 3, \dots, 10$  and  $t = 64, 128, \dots, 1024$ , the table shows the percentage of the runs (over 100) where the correct value was identified.

Range of $k$	Correct choice (percentage)									
	$t = 64$		$t = 128$		$t = 256$		$t = 512$		$t = 1024$	
	PPS	uniform	PPS	uniform	PPS	uniform	PPS	uniform	PPS	uniform
2-3	100%	66%	100%	56%	100%	57%	100%	71%	100%	85%
2-4	100%	1%	100%	2%	100%	3%	100%	31%	100%	72%
2-5	100%	0%	100%	0%	100%	6%	100%	25%	100%	64%
2-6	100%	0%	100%	2%	100%	4%	100%	28%	100%	50%
2-7	100%	2%	100%	1%	100%	5%	100%	20%	100%	53%
2-8	100%	3%	100%	2%	100%	5%	100%	13%	100%	53%
2-9	100%	2%	100%	1%	100%	7%	100%	25%	100%	53%
2-10	100%	1%	100%	3%	100%	5%	100%	19%	100%	57%

In third experiment, we compared the accuracy of the silhouette estimates computed by PPS-SILHOUETTE, uniform sampling, and simplified silhouette, on the real datasets HIGGS and Covertype, considering  $k = 5, 10$  and  $t = 64, 256, 1024$ . Table 3 reports the the maximum and average absolute errors of the silhouette estimates, over 100 runs, together with the values of the exact silhouette and of the simplified silhouette. Similarly to the case of the synthetic dataset, PPS-SILHOUETTE provides very accurate estimates already for  $t = 64$ , with an average error smaller than 0.03, and for  $t \geq 256$  it features an average error below 0.01. The variance is below  $10^{-3}$  in all cases. On these datasets, the uniform sampling algorithm also provides fairly accurate estimates (with variance  $< 10^{-3}$  in all cases). However, for no combination of  $k$  and  $t$  the average error of the uniform sampling algorithm is lower than the one of PPS-SILHOUETTE, while its maximum error is slightly better only in three out of twelve configurations. Also, the simplified silhouette displays poor accuracy, worse than the one of PPS-SILHOUETTE even with  $t = 64$ . Once again, this experiment confirms the superiority of our PPS-SILHOUETTE algorithm with respect to the two competitors.

We ran an experiment similar in spirit to the second experiment, to further test the capability of PPS versus uniform sampling of identifying the best granularity  $k$  when the same clustering algorithm is applied to a dataset with different values of  $k$ . Specifically, we ran  $k$ -medoids clustering on the same synthetic dataset of the second experiment, for all values of  $k$  in an interval  $[2, \ell]$ , with  $\ell \geq 3$ , and checked whether the best clustering (according to the exact silhouette) was identified using the silhouette estimations returned by PPS-SILHOUETTE and by the uniform sampling algorithm. We ran the experiment for  $\ell = 3, \dots, 10$ , and expected sample sizes  $t \in \{64, 128, 256, 512, 1024\}$ . For each combination of  $\ell$  and  $t$ , we considered 100 trials (corresponding to 100 estimates of the silhouette by the two algorithms). Table 4 displays the fraction of times the correct value of  $k$  was identified by the two algorithms. Strikingly, PPS-SILHOUETTE identified the correct value of  $k$  100% of the times, for every combination of  $k$  and  $t$ , confirming the reliability and consistency of the silhouette estimate even for small  $t$  (e.g., 64).

For what concerns the uniform sampling algorithm, Table 4 shows that, except for the range  $k \in \{2, 3\}$  or  $t = 1024$ , the algorithm leads to the wrong choice of  $k$  more than half of the times. In fact, when  $t \leq 256$ , the correct value of  $k$  is identified no more than 7% of the times, which is less than expected if a random choice among the considered values of  $k$  were made. The results clearly improve with  $t = 1024$ , but still the wrong value of  $k$  is identified at least 15% of the times, and close to 50% of the times in most cases. These results provide further evidence of the superiority of PPS sampling.

As mentioned in the main paper, we also conducted an experiment to assess the accuracy of the estimate returned by PPS-SILHOUETTE under squared Euclidean distances (which do not satisfy the triangle inequality). Thanks to the availability of the efficient Apache Spark routine that computes the exact value with subquadratic work, for this experiment we were able to consider a large instance of the synthetic dataset with  $n = 10^8$  points, together with two clustering granularities ( $k = 5, 10$ ). We ran PPS-SILHOUETTE with expected sample size  $t = 64$ . For  $k = 5$ , PPS-SILHOUETTE provides estimates with an average error smaller than 0.005 and a maximum error of 0.008, while for  $k = 10$  the average error is smaller than 0.058 and the maximum error is 0.069. These results show that our

PPS-SILHOUETTE algorithm can be used to provide accurate estimates of the silhouette with a limited number of samples even for squared Euclidean distances.

Overall, the results show that PPS-SILHOUETTE exhibits a high level of accuracy even for relatively small values of the expected sample size  $t$ . Since the total work performed by PPS-SILHOUETTE is  $O(nkt)$ , this implies that reliable estimates can be obtained in much less than the  $\Theta(n^2)$  work required by the exact computation.

### 3.5 Performance Evaluation

In this section, we report the results of several experiments aimed at comparing the distributed performance of the MapReduce implementation of PPS-SILHOUETTE against the one of MapReduce implementations of the uniform sampling and the Frahling-Sohler optimization baselines, and of the optimized Spark routine for squared distances, on very large datasets.

In the first experiment, we assessed the scalability of the MapReduce version of PPS-SILHOUETTE. For this experiment, we used four instances of the synthetic dataset (see Section 3.3) with  $n = 10^6, 10^7, 10^8, 10^9$  elements and  $k = 5$  clusters. We ran MapReduce implementation of PPS-SILHOUETTE with  $t = 64$  using  $w = 1, 2, 4, 8, 16$  workers (each on a single core). For the dataset with  $n = 10^9$  elements, we considered only  $w = 4, 8, 16$  since for lower levels of parallelism the local memory available to each core was not sufficient to process the  $n/w$  elements assigned to each worker. The results are shown in Figure 1. We observe that for the two largest datasets PPS-SILHOUETTE exhibits linear scalability. For  $n = 10^7$ , the algorithm still exhibits linear scalability for up to 8 workers, while there is a limited gain in using 16 workers. For  $n = 10^6$ , scalability is still noticeable, however, due to the relatively small size of the dataset, the behavior is less regular due to the stronger incidence of communication overheads and caching effects. Also, for a fixed number of workers, we observe that the algorithm scales linearly with the number of elements, in accordance with our theoretical analysis.

In successive experiments, we compared the running times of the MapReduce implementations of PPS-SILHOUETTE (with  $t = 64$ ) and of the baselines. We compared PPS-SILHOUETTE with uniform sampling algorithm and times showed that, as expected, uniform sampling is slightly faster (by 10 – 20% in all experiments), due to the absence of the probability calculation phase. This mild advantage of uniform sampling is however counterbalanced by its much lower level of accuracy, quantified in the previous section, for equal sample size. We compared PPS-SILHOUETTE with the exact computation based on the definition (DEF), and of the exact computation based on the Frahling and Sohler optimization (FS), with fixed, maximum degree of parallelism  $w = 16$ , and using the smallest dataset of the previous experiment, namely the one with  $n = 10^6$  elements. While DEF was stopped after 6000 seconds, FS completed the execution in 1135 seconds, and PPS-SILHOUETTE in 14 seconds, thus (more than) two orders of magnitude faster than DEF and FS. Also, we point out that PPS-SILHOUETTE was able to estimate the silhouette for a three orders of magnitude larger dataset ( $n = 10^9$ ) in 2433 seconds, which is about twice the time required by FS on the dataset with  $10^6$  elements. Considering the accuracy of the estimation provided by PPS-SILHOUETTE, assessed in the previous subsection, these comparisons provide evidence of its practicality.

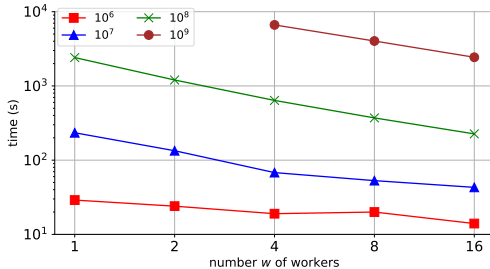


Figure 1: Running time (median over 5 runs) of our PPS-SILHOUETTE algorithm as function of the number  $w$  of workers, for datasets of different sizes.

Finally, we compared the performance of PPS-SILHOUETTE under squared Euclidean distances with the one of the optimized exact method available in Apache Spark for such distances, using our synthetic dataset with  $n = 10^8$  elements and two values of  $k$ , namely  $k = 5, 10$ . Since our goal in this experiment was to compare the best performance achievable by the two implementations, and since our PPS-SILHOUETTE algorithm provides very accurate estimates already with a limited number  $t$  of samples, we fixed  $t = 32$  and  $w = 16$  workers. For both values of  $k$  the estimates from PPS-SILHOUETTE are very precise (average error 0.007 for  $k = 5$  and 0.087 for  $k = 10$ ), while the running

time of PPS-SILHOUETTE is comparable to, even if higher than (up to approximately two times), the running time of the optimized Apache Spark method.

## 4 Conclusions

In this work, we developed the first efficient, sampling-based algorithm to estimate the silhouette coefficient for a given clustering with provable approximation guarantees, whose running time dramatically improves over the quadratic complexity required, in the general case, by the exact computation. We provided a distributed implementation of our algorithm in Map-Reduce which runs in constant rounds, and requires only sublinear space at each worker. The experimental evaluation conducted on real and synthetic datasets, demonstrates that our algorithm enables an accurate estimation of the silhouette for clusterings of massive datasets for which the exact computation is out of reach. Future research should target a more extensive experimentation on real-world datasets. Also, it would be interesting to devise a more flexible, dynamic version of the algorithm where the desired accuracy can be incrementally refined by reusing (part of) the previously sampled points.

## 5 Acknowledgments.

This work was supported, in part, by MIUR, the Italian Ministry of Education, University and Research, under PRIN Project n. 20174LF3T8 AHeAD (Efficient Algorithms for HARnessing Networked Data), and grant L. 232 (Dipartimenti di Eccellenza), and by the University of Padova under projects “STARS 2017: Algorithms for Inferential Data Mining” and “SID 2020: Resource-Allocation Tradeoffs for Dynamic and Extreme Data”. The authors want to thank Matteo Ceccarello for his invaluable help with the Apache Spark framework.

## References

- [1] T. Abeel, Y. V. d. Peer, and Y. Saeys. Java-ml: A machine learning library. *JMLR*, 2009.
- [2] C. C. Aggarwal and C. K. Reddy. *Data Clustering: Algorithms and Applications*, 2014.
- [3] P. Awasthi and M. Balcan. Center based clustering: A foundational perspective. In *Handbook of cluster analysis*, 2014.
- [4] B. Bahmani, B. Moseley, A. Vattani, R. Kumar, and S. Vassilvitskii. Scalable k-means++. *PVLDB* 2012.
- [5] M.-F. F. Balcan, S. Ehrlich, and Y. Liang. Distributed  $k$ -means and  $k$ -median clustering on general topologies. *NIPS* 2013.
- [6] A. Barger and D. Feldman.  $k$ -means for streaming and distributed big sparse data. *SDM* 2016.
- [7] P. Beame, P. Koutris, and D. Suciu. Communication steps for parallel query processing. *PODS* 2013.
- [8] M. Ceccarello, C. Fantozzi, A. Pietracaprina, G. Pucci, and F. Vandin. Clustering uncertain graphs. *PVLDB* 2017.
- [9] M. Ceccarello, A. Pietracaprina, and G. Pucci. Solving  $k$ -center clustering (with outliers) in MapReduce and streaming, almost as accurately as sequentially. *PVLDB* 2019.
- [10] S. Chechik, E. Cohen, and H. Kaplan. Average distance queries through weighted samples in graphs and metric spaces: high scalability with tight statistical guarantees. *APPROX/RANDOM* 2015.
- [11] E. Cohen, S. Chechik, and H. Kaplan. Clustering small samples with quality guarantees: adaptivity with one2all PPS. *AAAI* 2018.
- [12] J. Dean and S. Ghemawat. MapReduce: simplified data processing on large clusters. *Comm. ACM*.
- [13] A. Ene, S. Im, and B. Moseley. Fast clustering using MapReduce. *KDD* 2011.
- [14] D. Feldman and M. Langberg. A unified framework for approximating and clustering data. *STOC* 2011.
- [15] G. Frahling and C. Sohler. A fast  $k$ -means implementation using coresets. *Int. J. Comp. Geom. Appl.* 2008.
- [16] J. Han, J. Pei, and M. Kamber. *Data mining: concepts and techniques*, 2011.
- [17] C. Hennig, M. Meila, F. Murtagh, and R. Rocci. *Handbook of cluster analysis*, 2015.
- [18] M. S. Hossain and R. A. Angryk. Gdclust: A graph-based document clustering technique. *ICDMW 2007*.
- [19] E. R. Hruschka, L. N. de Castro, and R. J. Campello. Evolutionary algorithms for clustering gene-expression data. *ICDM* 2004.

- [20] H. J. Karloff, S. Suri, and S. Vassilvitskii. A model of computation for mapreduce. *SODA* 2010.
- [21] J. Leskovec, A. Rajaraman, and J. D. Ullman. *Mining of Massive Datasets*, 2020.
- [22] S. P. Lloyd. Least squares quantization in PCM. *IEEE Trans. on Information Theory*, 1982.
- [23] G. Malkomes, M. Kusner, W. Chen, K. Weinberger, and B. Moseley. Fast Distributed k-Center Clustering with Outliers on Massive Data. *NIPS* 2015.
- [24] A. Mazzetto, A. Pietracaprina, and G. Pucci. Accurate mapreduce algorithms for k-median and k-means in general metric spaces. *ISAAC* 2019.
- [25] D. Moulavi, P. A. Jaskowiak, R. J. G. B. Campello, A. Zimek, and J. Sander. Density-based clustering validation. *SDM* 2014.
- [26] R. Ng and J. Han. Efficient and effective clustering methods for spatial data mining. *VLDB* 1994.
- [27] A. Pietracaprina, G. Pucci, M. Riondato, F. Silvestri, and E. Upfal. Space-round tradeoffs for mapreduce computations. *ICS* 2012.
- [28] P. J. Rousseeuw. Silhouettes: a graphical aid to the interpretation and validation of cluster analysis. *J. of Comp. and App. Mathematics*, 1987.
- [29] T. Sellam, R. Cijvat, R. Koopmanschap, and M. Kersten. Blaeu: mapping and navigating large tables with cluster analysis. *PVLDB* 2016.
- [30] P. N. Tan, M. Steinbach, and V. Kumar. *Introduction to Data Mining*, 2016.
- [31] L. Lin, J. Ruoming, C. Aggarwal, and S. Yelong. Reliable clustering on uncertain graphs. *ICDM* 2012.
- [32] C. Tomasini, L. R. Emmendorfer, E. N. Borges, and K. S. Machado. A methodology for selecting the most suitable cluster validation internal indices. *SAC* 2016.
- [33] F. Wang, H.-H. Franco-Penya, J. D. Kelleher, J. Pugh, and R. Ross. An analysis of the application of simplified silhouette to the evaluation of k-means clustering validity. *MLDM* 2017.
- [34] C. Wiwie, J. Baumbach, and R. Röttger. Comparing the performance of biomedical clustering methods. *Nature methods*, 2015.
- [35] H. Xiong and Z. Li. Clustering validation measures. *Data Clustering: Algorithms and Applications*, 2014.